Electronically Excited States in Solution via a Smooth Dielectric Model Combined with Equation-of-Motion Coupled Cluster Theory

J. Coleman Howard,[†] James C. Womack,[‡] Jacek Dziedzic,[‡,¶] Chris-Kriton Skylaris,[‡] Benjamin P. Pritchard,[§] and T. Daniel Crawford[*,†]

[†]*Department of Chemistry, Virginia Tech, Blacksburg, VA 24061, USA*

[‡]*Department of Chemistry, University of Southampton, Highfield, Southampton SO17 1BJ, UK*

[¶]*Faculty of Applied Physics and Mathematics, Gdańsk University of Technology, Gdańsk 80-233, Poland*

[§]*Molecular Sciences Software Institute, Virginia Tech, Blacksburg, VA 24060, USA*

E-mail: crawdad@vt.edu

Abstract

We present a method for computing excitation energies for molecules in solvent, based on the combination of a minimal parameter implicit solvent model and the equation-of-motion coupled-cluster singles and doubles method (EOM-CCSD). In this method, the solvent medium is represented by a smoothly varying dielectric function, constructed directly from the quantum mechanical electronic density using only two tunable parameters. The solvent-solute electrostatic interactions are computed by numerical solution of the nonhomogeneous Poisson equation and incorporated at the Hartree-Fock stage of the EOM-CCSD calculation by modification of the electrostatic

potential. We demonstrate the method by computing excited state transition energies and solvent shifts for several small molecules in water. Results are presented for solvated H_2O, formaldehyde, acetone and *trans*-acrolein, which have low-lying $n \rightarrow \pi^*$ transitions and associated blue shifts in aqueous solution. Comparisons are made with experimental data and other theoretical approaches, including popular implicit solvation models and QM/MM methods. We find that our approach provides surprisingly good agreement with both experiment and the other models, despite its comparative simplicity. This approach only requires modification of the Fock operator and total energy expressions at the Hartree-Fock level—solvation effects enter into the EOM-CCSD calculation only through the Hartree-Fock orbitals. Our model provides a theoretically and computationally simple route for accurate simulations of excited state spectra of molecules in solution, paving the way for studies of larger and more complex molecules.

1 Introduction

The fundamental philosophy of quantum mechanical (QM) computational solvation models is that detailed information of a solvent environment can be reduced to a system with fewer degrees of freedom that still maintains the essential features relevant to chemical phenomena of interest. A layered computational approach is utilized, wherein the molecular solute is treated quantum mechanically. The description of the solvent layer and the coupling between the solute and solvent distinguishes the different solvation models. Explicit molecules comprising a solvent environment can be modeled by potentials as in molecular mechanics (MM) methods, leading to a QM/MM family of solvation models.[1,2] These methods can range in complexity with the simplest being a mechanical embedding of a quantum solute.[3] More sophisticated QM/MM approaches introduce point charges for the solvent molecules to polarize the QM solute via one-electron perturbations to the Hamiltonian.[4] Introducing polarization effects represents a further improvement in QM/MM methods. Polarizable embedding[5–8] (PE or MMpol) uses point dipoles to incorporate polarization into QM/MM calculations. Polarizable point dipoles are also used in the AMOEBA force field,[9,10] which has been employed to model the solvent layer in QM/MM implementations.[11,12] The effective fragment potential (EFP)[13] from Gordon and coworkers aims for high accuracy by deriving solvent potentials from *ab initio* calculations specifically for the solvent molecular geometry. Other polarizable QM/MM methods have used the fluctuating charge (FQ) approach[14,15] and the Drude oscillator model.[16,17]

An alternative to describing explicit QM solvent molecules with force fields is to model the solvent environment implicitly as a continuous medium, resulting in QM continuum solvation models.[18–20] The central idea in continuum solvation models is that a molecular solute system is positioned within a cavity surrounded by a dielectric medium representing the solvent. By this construction, continuum models include no explicit solvent-solvent interactions, unlike QM/MM approaches. The only solvent-related terms that enter the Hamiltonian directly are solvent-solute interactions. The physics of the solvation problem

in continuum methods can be summarized as finding the response of the dielectric medium to the solute's molecular charge distribution. The polarized medium also back-polarizes the solute, resulting in a mutual polarization of the QM solute and the solvent, which must be calculated in a self-consistent manner. An advantage of modeling the solvent in this manner is that it avoids the need to average over many configurations of a large number of explicit solvent molecules.

Continuum solvation models are characterized by their definition of the solute cavity and their representation of the dielectric. The electrostatic problem can then be cast as an appropriate formulation of the Poisson equation for a charge distribution in a medium with a defined dielectric permittivity and solute-solvent interface. Some of the most common QM continuum solvation models fall under the category of apparent surface charge (ASC) methods.[21–23] In ASC methods, the electrostatic problem is solved by finding polarization charges at points on a cavity surface. The polarization charges appear on the surface as a result of a step discontinuity in the permittivity at the boundary between the solute and the dielectric. These methods typically define a solute cavity to be composed of atom-centered spheres based on van der Waals radii, although other cavity definitions are used as well to better approximate the molecular shape. Among the most popular of these methods is the celebrated polarizable continuum model (PCM),[20,21,23,24] which has been applied successfully to compute a variety of molecular properties.[20] Another method in the ASC family which has been widely used is the conductor-like screening model (COSMO).[22,25] COSMO differs from the PCM approach by setting the permittivity outside of the cavity to that of a conductor and then scaling the resulting surface charges to obtain the effective polarization of a particular solvent, resulting in a simpler implementation relative to PCM. The treatment of nonelectrostatic interaction energy contributions also differs among particular implicit solvent model implementations, including terms for the cavity formation, dispersion and repulsion energies.[20]

In this work, we implement a continuum solvation model based on nonhomogeneous per-

mittivity, previously developed for use in plane-wave DFT calculations,[26–30] into a Hartree-Fock framework. This is a minimal parameter model where the solute cavity is defined by the isosurfaces of the electronic density. The electrostatic potential is obtained by direct solution of the nonhomogeneous Poisson equation in real space with a multigrid solver. This model is appealing due to its relative simplicity, its high accuracy[29] and its minimal parameter (more *ab initio*) character.

In this case, computing the electrostatics for a QM solute in a polarizable dielectric requires the total electrostatic potential in the presence of the solvent to be generated on a grid and transformed into a suitable representation for Hartree-Fock and subsequent correlated calculations. Here, we apply this solvation procedure to the computation of electronic excitation energies using the equation-of-motion coupled-cluster method,[31–33] restricted to single and double excitations (EOM-CCSD). For a small set of molecules, we calculate solvatochromic shifts for comparison with other QM solvation methods, as well as experimental data.

2 Theoretical Background

The present solvation model replaces the electrostatics of the Restricted Hartree-Fock (RHF) self-consistent field (SCF) procedure with the potential of a solute in a polarizable dielectric medium defined by a density-dependent permittivity. The electrostatics in this implicit solvent model are described by the nonhomogeneous Poisson Equation (NPE) (Equation 1).

$$\nabla \cdot \left[\epsilon(\mathbf{r})\nabla V^{\mathrm{NPE}}(\mathbf{r})\right] = -4\pi\rho_{\mathrm{tot}}(\mathbf{r}) \tag{1}$$

Here, ρ_{tot} includes the solute electronic and nuclear charges, and the permittivity ϵ is a smooth parameterized function of the solute electronic density, giving the total electrostatic potential V^{NPE}. This approach was introduced by Fattebert and Gygi[26,27] and further extended by Scherlis *et al.*,[28] Andreussi *et al.*[34] and Skylaris and coworkers[29,30,35] for use in

DFT calculations with a plane-wave-derived basis. Our implementation of this model within a Hartree-Fock framework utilizing atom-centered Gaussian basis sets follows, specifically, based upon the developments of Dziedzic *et al.*[29] for this solvation approach.

The parameterized form of the permittivity introduced by Fattebert and Gygi[26,27] is as follows:

$$\epsilon[\rho(\mathbf{r})] = 1 + \frac{\epsilon_\infty - 1}{2}\left[1 + \frac{1 - (\rho(\mathbf{r})/\rho_0)^{2\beta}}{1 + (\rho(\mathbf{r})/\rho_0)^{2\beta}}\right] \tag{2}$$

Here, ϵ as a function of the electron density ρ depends on the bulk solvent permittivity ϵ_∞, as well as the parameters ρ_0 and β. These parameters effectively define a solute cavity where $\epsilon = 1$ surrounded by a smooth transitioning region where the permittivity increases to its bulk value. In this work, we have adopted the values of 0.00055 a.u. for ρ_0 and 1.6 for β. This parameterization of the model has been shown to minimize the root-mean-square error of calculated DFT solvation free energies relative to experiment for a test set composed of a variety of solute molecules.[29] Since the permittivity evidently depends on the molecular orbitals, its variation should be included in the SCF procedure. However, selecting a fixed permittivity based on a reasonable initial density (e.g., a converged vacuum electronic density) is computationally less demanding and was shown to introduce negligible errors relative to a DFT calculation in which the cavity responds self-consistently with the electron density.[29]

To obtain the potential, V^{NPE}, we have implemented an interface between the Psi4 software package[36] and the Poisson equation solver in the DL_MG library.[37–40] DL_MG employs the multigrid technique[41,42] to solve forms of the Poisson-Boltzmann equation on a real-space grid, achieving efficiency through MPI + OpenMP hybrid parallelism. At each step of an SCF loop, the current total density is computed on a regular 3-dimensional grid for input to the Poisson solver. Since the total electrostatic potential of the solute in the

presence of solvent is the quantity of interest, the total density includes, in addition to the electronic density, the nuclear density represented as smeared charges in the form of tight Gaussian functions centered at the nuclei.[28,29] The Poisson solver obtains an initial V^{NPE} solution computing finite difference derivatives to 2nd order in accuracy, which can then be improved to effective higher orders of accuracy through the method of "defect correction." This technique employs higher order discretization of differential operators to iteratively improve upon the original second order solution.[30,43] In this work, we use DL_MG to obtain a defect-corrected 12^{th} order solution to the NPE.

Upon obtaining a solution for the total electrostatic potential, V^{NPE}, the potential is introduced into the Hamiltonian by a modification of the Fock matrix to include V^{NPE} numerically integrated into the atomic orbital (AO) basis. The Fock matrix $\mathbf{F}$ in the AO basis $\{\phi_m\}$ is composed of the usual terms for the kinetic energy and the exchange terms on the first two lines of Equation 3.

$$
\begin{aligned}
F_{mn} = & \int d\mathbf{r_1} \phi_m^*(\mathbf{r_1}) \left[-\frac{1}{2}\nabla^2 \right] \phi_n(\mathbf{r_1}) \\
& - \frac{1}{2} \sum_{ls} P_{ls} \int \int d\mathbf{r_1} d\mathbf{r_2} \; \phi_m^*(\mathbf{r_1}) \phi_l(\mathbf{r_1}) r_{12}^{-1} \phi_s^*(\mathbf{r_2}) \phi_n(\mathbf{r_2}) \\
& + \int d\mathbf{r_1} \; \phi_m^*(\mathbf{r_1}) V^{\mathrm{NPE}}(\mathbf{r_1}) \phi_n(\mathbf{r_1}) \\
& + \int d\mathbf{r_1} \; \phi_m^*(\mathbf{r_1}) \left[\sum_A \frac{-Z_A}{|\mathbf{r_1} - \mathbf{R}_A|} + \frac{Z_A}{|\mathbf{r_1} - \mathbf{R}_A|} \mathrm{erf}\left(\frac{|\mathbf{r_1} - \mathbf{R}_A|}{\sigma} \right) \right] \phi_n(\mathbf{r_1}).
\end{aligned}
\tag{3}
$$

Since the potential due to the smeared charges of the nuclei is already included in V^{NPE}, the last line of Equation 3 provides a correction by including the difference between the nuclear potential of point charges in vacuum and that of smeared Gaussian charges in vacuum.[30]

If we substitute the solution of the homogeneous Poisson equation for $V^{\mathrm{NPE}}(r_1)$, the

potential from the smeared nuclei on the last line is canceled and the vacuum Coulomb repulsion appears, bringing Equation 3 in line with the usual expression for the Fock matrix, albeit with the electrostatics computed numerically on a grid.

If the core Hamiltonian is defined as the sum of lines one and four from Equation 3, then the total energy is in a slightly different form than the usual RHF energy (Equation 4).

$$E_{\text{total}} = \frac{1}{2}\sum_{m,n} P_{mn}\left(H_{mn}^{\text{core}} + F_{mn}\right) + \frac{1}{2}\sum_{A,B}\left(\frac{Z_A Z_B}{R_{AB}} - \int\int d\mathbf{r}d\mathbf{r}'\ \frac{\rho_A(\mathbf{r})\rho_B(\mathbf{r}')}{|\mathbf{r}-\mathbf{r}'|}\right) + \frac{1}{2}\sum_{A}\int dr\rho_A(\mathbf{r})V^{\text{NPE}}(\mathbf{r}) \tag{4}$$

The term on the second line of Equation 4 represents the interaction energy of the smeared Gaussian charge densities, $\rho_A(\mathbf{r})$, and the total electrostatic potential, $V^{\text{NPE}}(\mathbf{r})$. When combined with the third term on the right of Equation 3 (summed over AOs and contracted with the density matrix, P_{mn}), this completes the interaction of the total charge density (electronic and smeared ion) with $V^{\text{NPE}}(\mathbf{r})$.

The usual point-charge representation of nuclear charges is restored in the total energy expression by the subtraction of interaction energies in the smeared ion representation and their replacement by the corresponding point-charge interaction energies. The double summation over nuclear centers on the first line of Equation 4 replaces the interaction between smeared Gaussian charges with the nuclear repulsion between point charges, while the interaction of the electronic density with smeared ions is replaced with the corresponding point charge interaction within F_{mn} (in the last line of Equation 3).

Since any solvation calculation requires a proper reference for a meaningful interpretation, an SCF procedure is first fully converged in vacuum using Equation 3. The total electrostatic potential is computed using DL_MG with unit permittivity at all grid points. This allows a more straightforward comparison with values computed in the presence of the dielectric. The converged vacuum electron density is used to construct the permittivity function for the

subsequent solvent calculation and, thus, fix the dielectric cavity for the duration of the solvent SCF procedure. For open boundary conditions, the Poisson solver requires electrostatic potential values for the boundary points of the grid, and these are calculated in Psi4 at each SCF iteration, with the approximation of a homogeneous dielectric equal to the solvent's bulk permittivity.

In this work, we apply this solvation procedure to the calculation of electronic excitation energies using the Equation-of-Motion Coupled-Cluster method,[31–33] restricted to single and double excitations (EOM-CCSD). The converged molecular orbitals and Fock matrix elements from the vacuum and solvent SCF procedures are used in correlated calculations to obtain excitation energies and, therefore, solvatochromic shifts. In this work, there is no further modification to the correlation model to account for solvation effects. The solvent could be coupled to the CCSD ground state density and/or to excited state densities, but the solvation effect here is limited to obtaining the Hartree-Fock reference state, an approach well understood for implicit models.[44] This approximation is analogous to the Perturbation Theory on the Energy (PTE)[24,44] approach to ground-state PCM calculations and frozen-reaction-field (FRF)[45] approximation to excited states. More advanced treatments of solute-continuum interactions in excited states have been developed for PCM to account for the effect of electron correlation on the solvent potential as well as the solvent response to electronic excitation.[45–47] Inclusion of nonequilibrium solvation effects, which, in the context of vertical electronic excitations, means that only the solvent's electronic degrees respond to the excitation, has been implemented in the PCM and SVPE implicit models.[20,46,48]

3 Computational Methods

EOM-CCSD excitation energies and associated oscillator strengths were computed combining the Psi4 Hartree-Fock implementation with the DL_MG Poisson solver for electrostatics and polarization in vacuum and with water as a solvent using the experimental value of 78.34

for the bulk permittivity for four solute molecules – H_2O, acetone, formaldehyde and *trans*-acrolein. Each of these molecules undergoes a shift in the electronic excitation spectrum when solvated in aqueous solution. The computations employed Dunning's double- and triple-ζ correlation-consistent basis sets, augmented with diffuse functions (aug-cc-pVDZ and aug-cc-pVTZ).[49] All geometries were optimized in vacuum with the B3LYP functional[50–52] and a double-ζ basis set with a set of d polarization functions for non-hydrogen atoms (6-31G*).[53] For each molecule, vacuum and solvent calculations used the same optimized geometry. The EOM-CCSD equations were solved for the two lowest roots of each irreducible representation of the molecular point group for each solute molecule. For the selection of the regular grids in the DL_MG solver, cubic grids were chosen that reproduce Psi4 EOM-CCSD vacuum excitations to within 0.05 eV (see Supporting Information for grid details).

4 Results and Discussion

4.1 H_2O Solvated in Water

A single H_2O molecule represents a convenient benchmarking case for the solvation model presented here. The electronic spectra for water in the gas and liquid phases are known experimentally and have been studied with a variety of theoretical approaches.[54–66] Table 1 presents the excitation energies for a single H_2O molecule computed with the EOM-CCSD method using the aug-cc-pVDZ and and aug-cc-pVTZ basis sets. For each basis set, the lowest two excitations corresponding to each irreducible representation of the final state symmetry (labeled in the 1st column) are reported in terms of the excitation energy and the oscillator strength of the transition (f) in parentheses. The 2nd and 4th columns of the table provide the vacuum values for these excitations, where the vacuum electrostatics are computed via numerical solution of the homogeneous Poisson equation through the DL_MG library. For each basis set, in the column following the vacuum values, the results are given for an H_2O molecule embedded in a dielectric medium to mimic an aqueous environment.

In the gas phase, peaks at 7.4 eV and 9.7 eV have been assigned to B_1 and A_1 states, corresponding to Rydberg transitions of the type n→3s and n→3p, respectively.[63] In the liquid phase, the B_1 transition is around 0.8 eV higher than the gas phase, while the A_1 state blue shifts less, by 0.2 eV.[56,58] The results on the first and third rows of Table 1 correspond to these excitations. The diffuse nature of the excited states in these Rydberg-type transitions requires the use of diffuse basis sets. Upon increasing the quality of the basis set from aug-cc-pVDZ to aug-cc-pVTZ, the excitation energies are seen to shift on the order of 0.1 to 0.4 eV. For the lowest state (1^1B_1), the double-ζ basis set is actually in better agreement with the experimental gas phase value, while the aug-cc-pVTZ calculation overestimates the excitation energy by just over 0.1 eV at 7.54 eV. The solvent shifts for both basis sets are underestimated for the lowest excitation, both predicting virtually identical shifts near 0.45 eV. For the lowest excited A_1 state (2^1A_1), the solvent shifts computed here are more

in line with experiment, with the EOM-CCSD calculations giving shifts of around 0.35 eV, a slight overestimation relative to experiment.

These results are in line with the vertical excitation energies computed at similar levels of theory, shown in Table 1. For those results, excitation energies have been computed in solution at the CCSD level of theory with the aug-cc-pVDZ and augmented triple-ζ basis sets using QM/MM (CCSD/MM) or continuum methodologies (CCSD-PCM). The reference vacuum values for these methods are near the double-ζ or triple-ζ values computed here, with geometric differences (and extra diffuse functions in the case of triple-ζ) resulting in excitation energy changes on the order of not more than hundredths of an eV. When available, the vacuum values are given in the footnotes of Table 1. The CCSD/MM results correspond to excitations computed within a linear response formalism[59,61,63] capturing solvent effects with a polarizable force field in an implementation of the combined coupled-cluster/molecular mechanics method (CC/MM). The MD (molecular dynamics) column corresponds to results obtained by averaging values over configurations of hundreds of MM waters, while the MS (mean structure) column data corresponds to a calculation on an average structure obtained from dynamics calculations. These excitation energies are in good agreement for the 1^1B_1 state, but the 2^1A_1 blue shift is too large relative to experiment, with the mean structure CCSD/MM calculation predicting a blue shift for this state larger than the computed shift for the 1^1B_1 state.

Both sets of EOM-CCSD solvent shifts computed here are close to those computed with sophisticated CCSD-PCM excitation calculations.[67,68] Solvent terms only enter the EOM-CCSD computations implicitly in the calculations presented here through their contributions to the Fock matrix, while the CCSD-PCM linear response (LR) and state-specific (SS) methods include solvent terms explicitly in the coupled-cluster equations and response function. These two CCSD-PCM methods give 1^1B_1 shifts of 0.54 and 0.36 eV and 2^1A_1 shifts of 0.39 eV and 0.26 eV, respectively. These methods correspond to the columns of Table 1 labeled LR and SS. In another column are the results of a "corrected" linear response PCM

method (c-LR) ,[69] which more accurately treats the excited state solute-solvent polarization than the LR implementation (the two are equivalent in vacuum). The ω_0 values in the last column of Table 1 correspond to PCM charges fixed to the ground state values within the excited state calculations.

The oscillator strength for this lowest excitation has an experimental value of 0.06.[58] The EOM-CCSD oscillator strength in water computed here is near 0.072 with the aug-cc-pVTZ basis set. The oscillator strengths computed with the CCSD/MM and CCSD-PCM methods compare relatively well, especially for this lowest excitation. For the 2^1A_1 transition, the oscillator strengths computed here with both basis sets also compare well to the CCSD-PCM value (0.122).

Table 1: Excitation energies (eV) for H_2O computed in vacuum and in water solvent with the EOM-CCSD method and values from experiment and previously reported at comparable levels of theory (with oscillator strengths in parentheses when available). The theoretical methods are described in the text

	aug-cc-pVDZ		aug-cc-pVTZ		Experiment[a]		CCSD/MM[b]		CCSD-PCM[c]			
	Vacuum	Solvent	Vacuum	Solvent	Gas	Solvent	MD	MS	SS	LR	c-LR	ω_0
1^1B_1	7.38 (.056)	7.82 (.076)	7.54 (.0523)	7.99 (.072)	7.4	8.2 (.06)	8.28 (.078)	8.18 (.079)	7.77	7.95 (.077)	7.78	7.99
1^1A_2	9.16 (.000)	9.56 (.000)	9.31 (.000)	9.72 (.000)	-	-	9.97 (.0057)	9.97 (.006)	9.34	9.73 (.000)	9.36	9.73
2^1A_1	9.82 (.105)	10.16 (.113)	9.92 (.100)	10.27 (.107)	9.7	9.9	10.45 (.025)	10.56 (.113)	10.10	10.23 (.122)	10.11	10.29
2^1B_1	11.05 (.001)	10.82 (.000)	10.78 (.003)	10.55 (.001)	-	-	10.22 (.0089)	-	10.83	11.06 (.000)	10.83	11.07
1^1B_2	11.57 (.021)	11.92 (.006)	11.66 (.019)	12.02 (.004)	-	-	-	-	11.67	12.05 (.011)	11.69	12.06
3^1A_1	11.73 (.000)	11.39 (.000)	11.34 (.001)	11.03 (.000)	-	-	10.70 (.079)	-	11.49	11.63 (.000)	11.49	11.65
2^1A_2	12.00 (.000)	12.55 (.000)	11.61 (.000)	12.07 (.000)	-	-	-	-	12.46	12.64 (.000)	12.48	12.65
2^1B_2	13.70 (.131)	13.81 (.126)	13.46 (.053)	13.68 (.061)	-	-	-	-	13.93	14.00 (.174)	13.94	14.08

[a]Reference 56

[b]References 63 and 61 (d-aug-cc-pVTZ basis set vacuum values: 7.62 eV (1^1B_1), 9.37 eV (1^1A_2) and 9.88 eV (2^1A_1))

[c]References 68 and 69 (aug-cc-pVDZ basis set vacuum values: 7.41 eV (1^1B_1) and 9.84 eV (2^1A_1))

4.2 Carbonyl Compounds Solvated in Water

The electronic excitation spectra of formaldehyde, acetone and *trans*-acrolein have drawn considerable interest for their low-lying n$\rightarrow \pi^*$ excitations, which undergo solvatochromic blue shifts in aqueous solution.[5,57,64,68,70–88] Table 2 presents the EOM-CCSD results for a single formaldehyde molecule. The lowest transition shown on the first row of data in Table 2 corresponds to the n$\rightarrow \pi^*$ transition, which has been the focus of many investigations.[5,64,71,75,76,78,79] The vacuum values for the double-ζ and triple-ζ basis sets are both in good agreement with the experimental value of 4.07 eV.[57] For the higher energy excitations, the vacuum EOM-CCSD values differ on the order of tenths of an eV. The excitation values differ between the aug-cc-pVDZ and aug-cc-pVTZ basis set from hundredths to tenths of an eV, depending on the nature of the transition. For example, the n$\rightarrow \pi^*$ valence transition is nearly identical between the two basis sets, while Rydberg transitions see larger deviations, similar to the results for H_2O.

The n$\rightarrow \pi^*$ excitation is slightly blue-shifted in aqueous solution to 4.28 eV.[71] The shifted n$\rightarrow \pi^*$ excitation energy is in good agreement for the EOM-CCSD solvent calculations in Table 2. Overall, this small experimental blue shift is overestimated by close to 0.1 eV in the present calculations. Kongsted *et al.*[76] have investigated the n$\rightarrow \pi^*$ transition in formaldehyde utilizing CCSD/MM calculations and found that a large sampling of solvent configurations is essential to reach a converged transition energy, which is nearly identical to the EOM-CCSD aug-cc-pVDZ value computed in solution here (Table 2). The need for such sampling is obviously avoided in an implicit solvent model, although the inclusion of specific solute-solvent interactions would likely improve the accuracy of the EOM-CCSD shifts (if properly averaged). In addition to the CCSD/MM n$\rightarrow \pi^*$ excitation, Table 2 presents micro-solvated CCSD computations for a series of solvated systems of one, two and four water molecules. While those values are not directly comparable to the CCSD/MM or the solvent calculations presented here, they are among the only results at the CCSD level, and capturing the intermolecular interactions at the full quantum level in this case leads

to shifts in very good agreement with the ≈0.2 eV shift seen in experiment. In addition to the lowest n→ π^* transition, the only other excitation with a shift larger than 0.1 eV is the transition to the 1^1B_1 state, another n→ π^* transition with a blue shift of 0.44 eV predicted here.

Table 3 collects the EOM-CCSD excitation energies and oscillator strengths for acetone. Experimentally, the n→ π^* transition occurs in the vapor phase around 4.5 eV[89,90] and is shifted to around 4.7 eV when solvated in water.[89,91–95] As can be seen in the first row for the aug-cc-pVDZ and aug-cc-pVTZ results in Table 3, the EOM-CCSD method accurately predicts the vapor excitation energy in the 1^1A_2 state corresponding to the n→ π^* excitation. The collection of experimental gas phase values in Table 3 indicate that the EOM-CCSD vacuum vertical excitation energies are in good agreement with the available measurements. The double-ζ values, in particular, compare (fortuitously) well with experiment, with only the 2^1B_2 excitation energy differing from the reference values by more than 0.1 eV. The basis-set dependence in acetone reflects the nature of the excited states, as with formaldehyde. The n→ π^* transition differs by only 0.01 eV from the aug-cc-pVDZ basis set to the aug-cc-pVTZ basis set, while the largest difference is 0.2 eV for the Rydberg transition to the 1^1B_2 state. The accuracy of the double-ζ basis set relative to the larger aug-cc-pVTZ basis set is a reflection of the nature of the transition, with the valence-type excitations apparently already well-described with the smaller basis set used here.

The implicit solvent model here overshifts the n→ π^* excitation relative to experiment, with a calculated blue shift in solution close to 0.3 eV with either basis set. Note that the symmetry of the transition makes it dipole-forbidden, even in solution for a solvent modeled strictly as a continuum. The CCSD/MM calculations of Aidas *et al.*[80] approaches in Table 3 results above predict a shift smaller than the experimental value, at around 0.14 eV. Explicit solvation of acetone with up to five H_2O molecules yields an n→ π^* excitation energy close to that computed in this work.[88] The CCSD-PCM methods in Table 3 predicted solvatochromic shifts close to the experimental value, all falling in the range of 4.62 eV to 4.66 eV for the

absolute energies. We note that a CC-in-DFT effort from Gomes *et al.*[81] utilizing CC2 in conjunction with embedded potentials from many averaged solvent configurations from molecular dynamics simulations successfully predicts the experimentally observed blue shift of 0.2 eV.

For the 1^1B_2 excitation on the second row of data in Table 3, the state-specific CCSD-PCM result is in good agreement with the double-ζ results computed here, differing by only 0.02 eV. In addition, the PCM oscillator strength of 0.047 can be compared to the value of 0.045 from the EOM-CCSD aug-cc-pVDZ solvent result from this work. For the higher-lying excitations, the EOM-CCSD aug-cc-pVDZ values in solvent are consistently larger compared to SS-CCSD-PCM, with the deviations increasing for the excitations near 9 eV to 0.2 and 0.3 eV.

Table 2: Excitation energies (eV) for formaldehyde computed in vacuum and in water solvent with the EOM-CCSD method and values from experiment and previously reported at comparable levels of theory (with oscillator strengths in parentheses when available). The theoretical methods are described in the text.

	aug-cc-pVDZ		aug-cc-pVTZ		Experiment[a]		CCSD/MM[c]	CCSD[d]		
	Vacuum	Solvent	Vacuum	Solvent	Gas[a]	Solvent[b]	MD	H_2O	$(H_2O)_2$	$(H_2O)_4$
1^1A_2	4.03 (.000)	4.32 (.000)	4.02 (.000)	4.31 (.000)	4.07	4.28	4.34	4.20	4.18	4.21
1^1B_2	7.03 (.022)	7.09 (.001)	7.23 (.022)	7.27 (.001)	7.11	-	-	-	-	-
2^1B_2	7.98 (.044)	8.03 (.068)	8.12 (.040)	8.17 (.065)	7.97	-	-	-	-	-
2^1A_1	8.05 (.060)	8.13 (.067)	8.22 (.056)	8.26 (.063)	8.14	-	-	-	-	-
2^1A_2	8.61 (.000)	8.64 (.000)	8.65 (.000)	8.64 (.000)	8.37	-	-	-	-	-
1^1B_1	9.41 (.001)	9.85 (.000)	9.32 (.001)	9.76 (.000)	-	-	-	-	-	-
3^1A_1	9.76 (.156)	9.82 (.135)	9.69 (.138)	9.76 (.137)	-	-	-	-	-	-
2^1B_1	10.90 (.042)	10.96 (.069)	11.00 (.042)	11.06 (.069)	-	-	-	-	-	-

[a]Reference 58
[b]Reference 71
[c]Reference 76 (aug-cc-pVTZ basis set vacuum value: 4.00 eV)
[d]Reference 75 (aug-cc-pVDZ basis set vacuum value: 4.01 eV)

Table 3: Excitation energies (eV) for acetone computed in vacuum and in water solvent with the EOM-CCSD method and values from experiment and previously reported at comparable levels of theory (with oscillator strengths in parentheses when available). The theoretical methods are described in the text.

	aug-cc-pVDZ		aug-cc-pVTZ		Experiment		CCSD/MM[e]	CCSD[f]	CCSD-PCM[g]			
	Vacuum	Solvent	Vacuum	Solvent	Gas	Solvent	MD	$(H_2O)_5$	SS	LR	c-LR	ω_0
1^1A_2	4.50 (.000)	4.78 (.000)	4.51 (.000)	4.80 (.000)	4.48[a]	4.69[a]	4.69	4.78	4.62	4.65 (.000)	4.63	4.66
1^1B_2	6.41 (.0324)	6.68 (.045)	6.61 (.031)	6.86 (.042)	6.36[b],6.35[c]	-	-	6.94	6.69	6.81 (.047)	6.71	6.82
2^1A_2	7.44 (.000)	7.81 (.000)	7.59 (.000)	7.91 (.000)	7.36[d],7.45[b]	-	-	-	7.72	7.95 (.000)	7.74	7.96
2^1A_1	7.46 (.000)	7.71 (.007)	7.63 (.000)	7.87 (.008)	7.41[d]	-	-	-	7.60	7.85 (.011)	7.62	7.85
2^1B_2	7.60 (.007)	7.72 (.000)	7.72 (.004)	7.85 (.000)	7.45[d]	-	-	-	7.69	7.88 (.001)	7.70	7.89
3^1A_1	8.23 (.069)	8.48 (.082)	8.36 (.063)	8.58 (.075)	-	-	-	-	8.36	8.60 (.188)	8.38	8.63
1^1B_1	8.49 (.016)	8.88 (.017)	8.56 (.013)	8.91 (.014)	-	-	-	-	8.68	9.01 (.019)	8.71	9.01
2^1B_1	9.33 (.002)	9.52 (.004)	9.26 (.000)	9.47 (.001)	-	-	-	-	9.23	9.22 (.002)	9.23	9.25

[a]Reference 89
[b]Reference 58
[c]Reference 94
[d]Reference 95
[e]Reference 80 (aug-cc-pVDZ basis set vacuum value: 4.55 eV)
[f]Reference 88 (aug-cc-pVDZ basis set vacuum values: 4.50 eV (1^1A_2) and 6.41 eV (1^1B_2))
[g]References 68 and 69 (aug-cc-pVDZ basis set vacuum value: 4.46 eV (1^1A_2))

The absorption spectrum of *trans*-acrolein features two absorption maxima which undergo solvent shifts in aqueous solution.[87,96–98] In addition to the $n \rightarrow \pi^*$ transition near 3.7 eV, which shifts to 3.94 eV in solution, a $\pi \rightarrow \pi^*$ excitation shifts lower in energy in water solvent, from around 6.4 eV to 5.9 eV. The vacuum excitation energies for these two transitions are in the first two rows of Table 4. The vacuum values here show larger deviations from experiments than seen for acetone. For either basis set, the predicted vacuum excitation energies are overestimated by 0.2 eV and more than 0.4 eV for the $n \rightarrow \pi^*$ and $\pi \rightarrow \pi^*$ transitions, respectively. However, even when setting aside the complications introduced by a solvent environment, comparing these vacuum values to the experiment must come with the usual caveats including that these are vertical excitation energies, and vibronic effects have not been considered. For the vacuum excitation energies, the results obtained with the two basis sets used in this work do not differ by more than 0.13 eV, with the two lowest-lying excitations agreeing to within 0.02 eV.

For the $n \rightarrow \pi^*$ excitation, the EOM-CCSD computations predict a blue shift of about 0.33 eV in solution, almost 0.1 eV larger than the experimental shift. The dielectric model here does correctly predict a red shift of the $\pi \rightarrow \pi^*$ excitation, although the 0.2 eV solvent shift is less than half that observed by experiment. Part of the discrepancy can be attributed to the use of the solute's vacuum geometry in the solvent calculations. CC and DFT computations have demonstrated that the $n \rightarrow \pi^*$ excitation energy is reduced in magnitude when employing an acrolein molecular geometry optimized in the presence of explicit waters and a PCM environment due to the sensitive nature of this excitation to the carbonyl bond length.[80] The solvent's ground state geometric effect on acrolein shifts can also be seen from the results of the PCM methods in Table 4. These computations utilize CCSD-PCM geometries, and the n$\rightarrow \pi^*$ shifts are close to 0.2 eV for any of the particular PCM implementations, in good agreement with the measured values. Both of the CCSD/MM shifts reported by Aidas *et al.*[87] are in good agreement with experiment, with the $\pi \rightarrow \pi^*$ red shift just slightly underestimated.

For these three molecules, we have also investigated the effects of short-range hydrogen bonding interactions which are absent in continuum solvation calculations. The dielectric model was combined with explicitly hydrated structures to compute solvatochromic shifts at the EOM-CCSD/aug-cc-pVDZ level. Excitation energies were computed for minimum-energy geometries of each compound with a single water molecule. These calculations should not be expected to improve comparisons to experimental values since a proper accounting of the interactions in the first solvation shell requires sampling over many configurations for each molecule to obtain statistically converged excitation energies. In fact, the addition of a single *ab initio* water molecule increases the n$\rightarrow \pi^*$ blue shift in each case, moving the n$\rightarrow \pi^*$ transition energy further away from the experimental value. The 0.28 eV dielectric shift in formaldehyde relative to the isolated molecule increases to 0.38 eV with the addition of an H_2O molecule. For acetone and acrolein, the 0.28 eV and 0.32 eV n$\rightarrow \pi^*$ blue shifts, respectively, increase to 0.37 eV and 0.39 eV. For the $\pi \rightarrow \pi^*$ red shift in acrolein, the magnitude of the shift is also increased relative to the calculation with only the dielectric solvent, in this case representing an improvement over the underestimated dielectric shift (-0.25 eV vs. -0.14 eV with the aug-cc-pVDZ basis set). Geometries, excitation energies and oscillator strengths for these calculations can be found in the Supporting Information.

Table 4: Excitation energies (eV) for acrolein computed in vacuum and in water solvent with the EOM-CCSD method and values from experiment and previously reported at comparable levels of theory (with oscillator strengths in parentheses when available). The theoretical methods are described in the text.

	aug-cc-pVDZ		aug-cc-pVTZ		Experiment		CCSD/MM[e]	CCSD[f]		CCSD-PCM[g]		
	Vacuum	Solvent	Vacuum	Solvent	Gas	Solvent	MD	$(H_2O)_5$	SS	LR	c-LR	ω_0
$1^1A''$	3.89 (.000)	4.21 (.000)	3.89 (.000)	4.22 (.000)	3.69[a],3.71[b]	3.94[c]	4.16	4.18	4.05	4.10 (.000)	4.06	4.11
$2^1A'$	6.84 (.221)	6.70 (.479)	6.86 (.396)	6.66 (.488)	6.41[b]	5.90[d]	6.54	6.61	6.54	6.39 (.549)	6.56	6.62
$3^1A'$	7.08 (.299)	7.06 (.029)	7.21 (.123)	7.24 (.018)	-	-	-	-	7.12	7.23 (.016)	7.13	7.25
$2^1A''$	7.18 (.000)	7.56 (.001)	7.25 (.000)	7.59 (.001)	-	-	-	-	7.38	7.48 (.000)	7.41	7.49

[a]Reference 87
[b]Reference 96
[c]Reference 54
[d]Reference 98
[e]Reference 87 (aug-cc-pVDZ basis set vacuum values: 3.93 eV ($1^1A''$) and 6.89 eV ($2^1A'$))
[f]Reference 88 (aug-cc-pVDZ basis set vacuum values: 3.88 eV ($1^1A''$) and 6.85 eV ($2^1A'$))
[g]References 68 and 69 (aug-cc-pVDZ basis set vacuum values: 3.88 eV ($1^1A''$) and 6.80 eV ($2^1A'$))

The solvatochromic blue shifts in these molecules can be rationalized by the differences in dipoles found in the ground and excited states. The $n \rightarrow \pi^*$ excitation energy shifts are summarized by Table 5, along with the associated dipole moments for the ground and excited states in vacuum and solution. For all three molecules, the differences in the ground state dipole moments (μ^{gs}) and excited state dipole moments (μ^{ex}) are roughly the same in vacuum and solution. The larger magnitude of the ground state dipole moment relative to the excited state in each molecule leads to a larger electrostatic interaction for the ground state and the associated blue shift seen in solvent. In the Onsager model, this blue shift is proportional to $\mu^{\mathrm{gs}} \cdot (\mu^{\mathrm{gs}} - \mu^{\mathrm{ex}})$.[99] The first and third columns of data in Table 5 demonstrate that the μ^{gs} values are significantly increased by the presence of the dielectric. The computed dipole moments for acetone in solution are very similar to those predicted by CC/MM calculations[87] with the polarizable SPCpol potential, within 0.1 D, while the formaldehyde dipole moments are smaller here by 0.3 D – 0.4 D.[76] The largest change in dipole moment due to the presence of dielectric here is for acrolein in water, where the ground and excited state dipole moments are increased by between 1.6 and 1.7 D with the aug-cc-pVTZ basis set.

Table 5: EOM-CCSD n$\rightarrow \pi^*$ ground and excited state dipole moments (D) in vacuum and solution and excitation energy shifts in solution (eV) computed with the aug-cc-pVTZ basis set

	Vacuum		Solvent		
	μ^{gs}	μ^{ex}	μ^{gs}	μ^{ex}	ΔE_{ex}
Formaldehyde	2.39	1.17	3.49	2.29	0.28
Acetone	2.96	1.51	4.40	3.00	0.29
Acrolein	3.18	0.60	4.86	2.22	0.33

5 Conclusions

We have presented a method for computing excited state energies of molecules in the presence of solvent based on the EOM-CCSD method. The emphasis of our work was to include the effects of the solvent in a simple and efficient way. To this end, we implemented a smooth, polarizable continuum model within a Hartree-Fock framework, utilizing an interface to the DL_MG multigrid real-space solver library to capture all electrostatic interactions through numerical solution of the non-homogeneous Poisson equation. SCF orbitals for the cases of vacuum permittivity and bulk water permittivity are used in subsequent coupled-cluster calculations to model solvatochromic shifts for vertical electronic excitation energies with the EOM-CCSD method.

For the molecules of water, formaldehyde, acetone and *trans*-acrolein, our model reliably reproduces all experimental shifts in aqueous solution. For the low-lying n$\rightarrow \pi^*$ blue shifts, the EOM-CCSD results differ from experimental measures by around 0.1 eV, while the shifts predicted for the Rydberg-type transitions in solvated water deviate slightly more from experiment, by as much as 0.3 eV. Both excitation energies as well as oscillator strengths computed here with the EOM-CCSD method compare well to other contemporary solvation models, including QM/MM and continuum techniques. The major advantages of our approach are that (i) it is simple to implement as the solvent effect on EOM-CCSD portion of calculation is purely via Hartree-Fock orbitals (no modification of the post-HF method is necessary), and (ii) it does not require explicit modeling of solvent molecules or solvent-solvent interactions, which is computationally less demanding and avoids dealing with the averaging of solvent degrees-of-freedom.

6 Acknowledgments

This research was supported by a grant (ACI-1450169) from the U.S. National Science Foundation and a HASI grant from the U.S. Department of Defense High Performance Comput-

ing Modernization Program. T.D.C. and J.C.H. acknowledge Advanced Research Computing at Virginia Tech for providing computational resource and technical support that have contributed to the results reported within the paper. J.C.W., J.D. and C.K.S. gratefully acknowledge funding under the embedded CSE program of the ARCHER UK National Supercomputing Service (http://www.archer.ac.uk), which has supported the development of the DL_MG multigrid solver library, and the EPSRC grant EP/J015059/1.

7 Supporting Information

A summary of grid sizes utilized in the calculations can be found in the Supporting Information, as well as optimized geometries, excitation energies and oscillator strengths for all micro-solvated structures. This information is available free of charge via the Internet at http://pubs.acs.org.

References

(1) Lin, H.; Truhlar, D. G. QM/MM: What Have We Learned, Where are We, and Where Do We Go from Here? *Theor. Chem. Acc.* **2006**, *117*, 185–199.

(2) Senn, H. M.; Thiel, W. QM/MM Methods for Biomolecular Systems. *Angew. Chem. Int. Ed. Engl.* **2009**, *48*, 1198–1229.

(3) Bakowies, D.; Thiel, W. Hybrid Models for Combined Quantum Mechanical and Molecular Mechanical Approaches. *J. Phys. Chem.* **1996**, *100*, 10580–10594.

(4) Field, M. J.; Bash, P. A.; Karplus, M. A Combined Quantum-Mechanical and Molecular Mechanical Potential for Molecular-Dynamics Simulations. *J. Comput. Chem.* **1990**, *11*, 700–733.

(5) Thompson, M. A. QM/MMpol: A Consistent Model for Solute/Solvent Polarization.

Application to the Aqueous Solvation and Spectroscopy of Formaldehyde, Acetaldehyde, and Acetone. *J. Phys. Chem.* **1996**, *100*, 14492–14507.

(6) Curutchet, C.; Munoz-Losa, A.; Monti, S.; Kongsted, J.; Scholes, G. D.; Mennucci, B. Electronic Energy Transfer in Condensed Phase Studied by a Polarizable QM/MM Model. *J. Chem. Theory Comput.* **2009**, *5*, 1838–1848.

(7) Olsen, J. M.; Aidas, K.; Kongsted, J. Excited States in Solution through Polarizable Embedding. *J. Chem. Theory Comput.* **2010**, *6*, 3721–3734.

(8) Daday, C.; Curutchet, C.; Sinicropi, A.; Mennucci, B.; Filippi, C. Chromophore-Protein Coupling beyond Nonpolarizable Models: Understanding Absorption in Green Fluorescent Protein. *J. Chem. Theory Comput.* **2015**, *11*, 4825–4839.

(9) Ponder, J. W.; Wu, C.; Ren, P.; Pande, V. S.; Chodera, J. D.; Schneiders, M. J.; Haque, I.; Mobley, D. L.; Lambrecht, D. S.; DiStasio Jr., R. A.; Head-Gordon, M.; Clark, G. N. I.; Johnson, M. E.; Head-Gordon, T. Current Status of the AMOEBA Polarizable Force Field. *J. Phys. Chem. B* **2010**, *114*, 2549–2564.

(10) Ren, P.; Wu, C.; Ponder, J. W. Polarizable Atomic Multipole-based Molecular Mechanics for Organic Molecules. *J. Chem. Theory Comput.* **2011**, *7*, 3143–3161.

(11) Loco, D.; Polack, É.; Caprasecca, S.; Lagardère, L.; Lipparini, F.; Piquemal, J.-P.; Mennucci, B. A QM/MM Approach Using the AMOEBA Polarizable Embedding: From Ground State Energies to Electronic Excitations. *J. Chem. Theory Comput.* **2016**, *12*, 3654–3661.

(12) Dziedzic, J.; Mao, Y.; Shao, Y.; Ponder, J.; Head-Gordon, T.; Head-Gordon, M.; Skylaris, C.-K. TINKTEP: A Fully Self-Consistent, Mutually Polarizable QM/MM Approach Based on the AMOEBA Force Field. *J. Chem. Phys.* **2016**, *145*, 124106.

(13) Gordon, M. S.; Freitag, M. A.; Bandyopadhyay, P.; Jensen, J. H.; Kairys, V.; Stevens, W. J. The Effective Fragment Potential Method: A QM-Based MM Approach to Modeling Environmental Effects in Chemistry. *J. Phys. Chem. A* **2001**, *105*, 293–307.

(14) Rick, S. W.; Stuart, S. J. In *Reviews in Computational Chemistry*; Lipowitz, K. B., Boyd, D. B., Eds.; Wiley, 2003; Vol. 18; pp 89–146.

(15) Lipparini, F.; Barone, V. Polarizable Force Fields and Polarizable Continuum Model: A Fluctuating Charges/PCM Approach. 1. Theory and Implementation. *J. Chem. Theory Comput.* **2011**, *7*, 3711–3724.

(16) Lamoureux, G.; Roux, B. Modeling Induced Polarization with Classical Drude Oscillators: Theory and Molecular Dynamics Simulation Algorithm. *J. Chem. Phys.* **2003**, *119*, 3025–3039.

(17) Boulanger, E.; Thiel, W. Solvent Boundary Potentials for Hybrid QM/MM Computations Using Classical Drude Oscillators: A Fully Polarizable Model. *J. Chem. Theory Comput.* **2012**, *8*, 4527–4538.

(18) Cramer, C. J.; Truhlar, D. G. Implicit Solvation Models: Equilibria, Structure, Spectra, and Dynamics. *Chem. Rev.* **1999**, *99*, 2161–2200.

(19) Orozco, M.; Luque, F. J. Theoretical Methods for the Description of the Solvent Effect in Biomolecular Systems. *Chem. Rev.* **2000**, *100*, 4187–4225.

(20) Tomasi, J.; Mennucci, B.; Cammi, R. Quantum Mechanical Continuum Solvation Models. *Chem. Rev.* **2005**, *105*, 2999–3093.

(21) Miertuš, S.; Scrocco, E.; Tomasi, J. Electrostatic Interaction of a Solute with a Continuum - a Direct Utilization of Ab Initio Molecular Potentials for the Prevision of Solvent Effects. *Chem. Phys.* **1981**, *55*, 117–129.

(22) Klamt, A.; Schüürmann, G. Cosmo - a New Approach to Dielectric Screening in Solvents with Explicit Expressions for the Screening Energy and Its Gradient. *J. Chem. Soc. Perkin Trans. 2* **1993**, 799–805.

(23) Tomasi, J.; Mennucci, B.; Cancès, E. The IEF Version of the PCM Solvation Method: An Overview of a New Method Addressed to Study Molecular Solutes at the QM Ab Initio Level. *J. Mol. Struct. (THEOCHEM)* **1999**, *464*, 211–226.

(24) Cammi, R. *Molecular Response Functions for the Polarizable Continuum Model*; SpringerBriefs in Molecular Science; Springer: Cham, 2013.

(25) Klamt, A. Conductor-Like Screening Model for Real Solvents - A New Approach to the Quantitative Calculation of Solvation Phenomena. *J. Phys. Chem.* **1995**, *99*, 2224–2235.

(26) Fattebert, J. L.; Gygi, F. Density Functional Theory for Efficient Ab Initio Molecular Dynamics Simulations in Solution. *J. Comput. Chem.* **2002**, *23*, 662–666.

(27) Fattebert, J. L.; Gygi, F. First-Principles Molecular Dynamics Simulations in a Continuum Solvent. *Int. J. Quantum Chem.* **2003**, *93*, 139–147.

(28) Scherlis, D. A.; Fattebert, J. L.; Gygi, F.; Cococcioni, M.; Marzari, N. A Unified Electrostatic and Cavitation Model for First-Principles Molecular Dynamics in Solution. *J. Chem. Phys.* **2006**, *124*, 74103.

(29) Dziedzic, J.; Helal, H. H.; Skylaris, C.-K.; Mostofi, A. A.; Payne, M. C. Minimal Parameter Implicit Solvent Model for Ab Initio Electronic-Structure Calculations. *EPL* **2011**, *95*, 43001.

(30) Dziedzic, J.; Fox, S. J.; Fox, T.; Tautermann, C. S.; Skylaris, C.-K. Large-scale DFT Calculations in Implicit Solvent - A Case Study on the T4 Lysozyme L99A/M102Q Protein. *Int. J. Quantum Chem.* **2013**, *113*, 771–785.

(31) Sekino, H.; Bartlett, R. J. A Linear Response, Coupled-Cluster Theory for Excitation-Energy. *Int. J. Quantum Chem.* **1984**, 255–265.

(32) Stanton, J. F.; Bartlett, R. J. The Equation of Motion Coupled-Cluster Method - a Systematic Biorthogonal Approach to Molecular Excitation Energies, Transition Probabilities, and Excited State Properties. *J. Chem. Phys.* **1993**, *98*, 7029–7039.

(33) Krylov, A. I. Equation-of-Motion Coupled-Cluster Methods for Open-Shell and Electronically Excited Species: The Hitchhiker's Guide to Fock Space. *Annu. Rev. Phys. Chem.* **2008**, *59*, 433–462.

(34) Andreussi, O.; Dabo, I.; Marzari, N. Revised Self-Consistent Continuum Solvation in Electronic-Structure Calculations. *J. Chem. Phys.* **2012**, *136*, 064102.

(35) Fox, S. J.; Dziedzic, J.; Fox, T.; Tautermann, C. S.; Skylaris, C.-K. Density Functional Theory Calculations on Entire Proteins for Free Energies of Binding: Application to a Model Polar Binding Site. *Proteins: Struct., Funct., Bioinf.* **2014**, *82*, 3335–3346.

(36) Parrish, R. M.; Burns, L. A.; Smith, D. G. A.; Simmonett, A. C.; DePrince, A. E.; Hohenstein, E. G.; Bozkaya, U.; Sokolov, A. Y.; Di Remigio, R.; Richard, R. M.; Gonthier, J. F.; James, A. M.; McAlexander, H. R.; Kumar, A.; Saitow, M.; Wang, X.; Pritchard, B. P.; Verma, P.; Schaefer, H. F.; Patkowski, K.; King, R. A.; Valeev, E. F.; Evangelista, F. A.; Turney, J. M.; Crawford, T. D.; Sherrill, C. D. Psi4 1.1: An Open-Source Electronic Structure Program Emphasizing Automation, Advanced Libraries, and Interoperability. *J. Chem. Theory Comput.* **2017**, *13*, 3185–3197.

(37) Anton, L.; Dziedzic, J.; Skylaris, C.-K.; Probert, M. I. J. Multigrid Solver Module for ONETEP, CASTEP and Other Codes (dCSE, 2013). (Technical report from dCSE project, available here: http://www.hector.ac.uk/cse/distributedcse/reports/onetep/).

(38) Skylaris, C.-K.; Dziedzic, J.; Anton, L. A Pinch of Salt in ONETEPs Sol-

vent Model (eCSE, 2014). (Technical report from eCSE project, available here: http://www.archer.ac.uk/community/eCSE/eCSE01-004/eCSE01-004.php).

(39) DL_MG website (hosted on CCPForge repository): https://ccpforge.cse.rl.ac.uk/gf/project/dl-mg/.

(40) Womack, J.C.; Anton, L.; Dziedzic, J.; Hasnip, P.J.; Probert, M I. J.; Skylaris, C.-K. Implementation and optimisation of advanced solvent modelling functionality in CASTEP and ONETEP (eCSE, 2016). (Technical report from eCSE project, to be released).

(41) Brandt, A. Multi-Level Adaptive Solutions to Boundary- Value Problems. *Math. Comp.* **1977**, 333–390.

(42) Merrick, M. P.; Iyer, K. A.; Beck, T. L. Multigrid Method for Electrostatic Computations in Numerical Density Functional Theory. *J. Phys. Chem.* **1995**, 12478.

(43) Schaffer, S. Higher Order Multigrid Methods. *Math. Comp.* **1984**, *43*, 89–115.

(44) Lipparini, F.; Mennucci, B. Perspective: Polarizable Continuum Models for Quantum-Mechanical Descriptions. *J. Chem. Phys.* **2016**, *144*, 160901.

(45) Caricato, M. Exploring Potential Energy Surfaces of Electronic Excited States in Solution with the EOM-CCSD-PCM Method. *J. Chem. Theory Comput.* **2012**, *8*, 5081–5091.

(46) Caricato, M. Absorption and Emission Spectra of Solvated Molecules with EOM-CCSD-PCM Method. *J. Chem. Theory Comput.* **2012**, *8*, 4494–4502.

(47) Caricato, M.; Lipparini, F.; Scalmani, G.; Cappelli, C.; Barone, V. Vertical Electronic Excitations in Solution with the EOM-CCSD Method Combined with a Polarizable Explicit/Implicit Solvent Model. *J. Chem. Theory Comput.* **2013**, *9*, 3035–3042.

(48) Chipman, D. M. Vertical Electronic Excitation with a Dielectric Continuum Model of Solvation Including Volume Polarization. I. Theory. *J. Chem. Phys.* **2009**, *131*, 014103.

(49) Kendall, R. A.; Dunning, T. H.; Harrison, R. J. Electron-Affinities of the 1st-Row Atoms Revisited - Systematic Basis-Sets and Wave-Functions. *J. Chem. Phys.* **1992**, *96*, 6796–6806.

(50) Becke, A. D. Density-Functional Thermochemistry. III. The Role of Exact Exchange. *J. Chem. Phys.* **1993**, *98*, 5648–5652.

(51) Lee, C. T.; Yang, W. T.; Parr, R. G. Development of the Colle-Salvetti Correlation-Energy Formula into a Functional of the Electron-Density. *Phys. Rev. B* **1988**, *37*, 785–789.

(52) Stephens, P. J.; Devlin, F. J.; Chabalowski, C. F.; Frisch, M. J. Ab-Initio Calculation of Vibrational Absorption and Circular-Dichroism Spectra Using Density-Functional Force-Fields. *J. Phys. Chem.* **1994**, *98*, 11623–11627.

(53) Hariharan, P. C.; Pople, J. A. Influence of Polarization Functions on Molecular-Orbital Hydrogenation Energies. *Theor. Chim. Acta* **1973**, *28*, 213–222.

(54) Mackinney, G.; Temmer, O. The Deterioration of Dried Fruit. IV. Spectrophotometric and Polarographic Studies. *J. Am. Chem. Soc.* **1948**, *70*, 3586–3590.

(55) Moskvin, A.; Yablonskii, O. P.; Bondar, L. F. An Experimental Investigation of the Effect of Alkyl Substituents on the Position of the K and R Absorption Bands in Acrolein Derivatives. *Theor. Exp. Chem.* **1966**, *2*, 469–482.

(56) Kerr, G. D.; Williams, M. W.; Birkhoff, R. D.; Hamm, R. N.; Painter, L. R. Optical and Dielectric Properties of Water in Vacuum Ultraviolet. *Phys. Rev. A* **1972**, *5*, 2523–2527.

(57) Robin, M. B. *Higher Excited States of Polyatomic Molecules*; Academic Press: New York, 1974.

(58) Robin, M. B. *Higher Excited States of Polyatomic Molecules*; Academic Press: New York, 1985.

(59) Christiansen, O.; Nymand, T. M.; Mikkelsen, K. V. A Theoretical Study of the Electronic Spectrum of Water. *J. Chem. Phys.* **2000**, *113*, 8101–8112.

(60) Jensen, L.; van Duijnen, P. T.; Snijders, J. G. A Discrete Solvent Reaction Field Model within Density Functional Theory. *J. Chem. Phys.* **2003**, *118*, 514–521.

(61) Kongsted, J.; Osted, A.; Mikkelsen, K. V.; Christiansen, O. Linear Response Functions for Coupled Cluster/Molecular Mechanics including Polarization Interactions. *J. Chem. Phys.* **2003**, *118*, 1620–1633.

(62) Jacob, C. R.; Neugebauer, J.; Jensen, L.; Visscher, L. Comparison of Frozen-Density Embedding and Discrete Reaction Field Solvent Models for Molecular Properties. *Phys. Chem. Chem. Phys.* **2006**, *8*, 2349–2359.

(63) Osted, A.; Kongsted, J.; Mikkelsen, K. V.; Åstrand, P. O.; Christiansen, O. Statistical Mechanically Averaged Molecular Properties of Liquid Water Calculated Using the Combined Coupled Cluster/Molecular Dynamics Method. *J. Chem. Phys.* **2006**, *124*, 124503.

(64) Paterson, M. J.; Kongsted, J.; Christiansen, O.; Mikkelsen, K. V.; Nielsen, C. B. Two-Photon Absorption Cross Sections: An Investigation of Solvent Effects. Theoretical Studies on Formaldehyde and Water. *J. Chem. Phys.* **2006**, *125*, 184501.

(65) Höfener, S.; Gomes, A. S. P.; Visscher, L. Molecular Properties via a Subsystem Density Functional Theory formulation: A Common Framework for Electronic Embedding. *J. Chem. Phys.* **2012**, *136*.

(66) Höfener, S.; Gomes, A. S.; Visscher, L. Solvatochromic Shifts from Coupled-Cluster Theory Embedded in Density Functional Theory. *J. Chem. Phys.* **2013**, *139*, 104106.

(67) Caricato, M.; Scalmani, G.; Trucks, G. W.; Frisch, M. J. Coupled Cluster Calculations in Solution with the Polarizable Continuum Model of Solvation. *J. Phys. Chem. Lett.* **2010**, *1*, 2369–2373.

(68) Caricato, M. A Comparison between State-Specific and Linear-Response Formalisms for the Calculation of Vertical Electronic Transition Energy in Solution with the CCSD-PCM Method. *J. Chem. Phys.* **2013**, *139*, 044116.

(69) Caricato, M. A Corrected-Linear Response Formalism for the Calculation of Electronic Excitation Energies of Solvated Molecules with the CCSD-PCM Method. *Computational and Theoretical Chemistry* **2014**, *1040–1041*, 99–105.

(70) Mentall, J. E.; Gentieu, E. P.; Krauss, M.; Neumann, D. Photoionization and Absorption Spectrum of Formaldehyde in Vacuum Ultraviolet. *J. Chem. Phys.* **1971**, *55*, 5471–5479.

(71) Bercovici, T.; Becker, R. S.; King, J. Formaldehyde - Comprehensive Spectral Investigation as a Function of Solvent and Temperature. *J. Chem. Phys.* **1972**, *56*, 3956–3963.

(72) Lessard, C. R.; Moule, D. C. Assignment of Rydberg Transitions in Electronic Absorption-Spectrum of Formaldehyde. *J. Chem. Phys.* **1977**, *66*, 3908–3916.

(73) Gwaltney, S. R.; Bartlett, R. J. An Application of the Equation-of-Motion Coupled-Cluster Method to the Excited-States of Formaldehyde, Acetaldehyde, and Acetone. *Chem. Phys. Lett.* **1995**, *241*, 26–32.

(74) Wiberg, K. B.; de Oliveira, A. E.; Trucks, G. A Comparison of the Electronic Transition Energies for Ethene, Isobutene, Formaldehyde, and Acetone Calculated Using RPA, TDDFT, and EOM-CCSD. Effect of Basis Sets. *J. Phys. Chem. A* **2002**, *106*, 4192–4199.

(75) Kongsted, J.; Osted, A.; Pedersen, T. B.; Mikkelsen, K. V.; Christiansen, O. The $n \rightarrow \pi^*$ Electronic Transition in Microsolvated Formaldehyde. A Coupled Cluster and Combined Coupled Cluster/Molecular Mechanics Study. *J. Phys. Chem. A* **2004**, *108*, 8624–8632.

(76) Kongsted, J.; Osted, A.; Mikkelsen, K. V.; Åstrand, P. O.; Christiansen, O. Solvent Effects on the $n \rightarrow \pi^*$ Electronic Transition in Formaldehyde: A Combined Coupled Cluster/Molecular Dynamics Study. *J. Chem. Phys.* **2004**, *121*, 8435–8445.

(77) Xu, Z. R.; Matsika, S. Combined Multireference Configuration Interaction/Molecular Dynamics Approach for Calculating Solvatochromic Shifts: Application to the $n_O \rightarrow \pi^*$ Electronic Transition of Formaldehyde. *J. Phys. Chem. A* **2006**, *110*, 12035–12043.

(78) Slipchenko, L. V. Solvation of the Excited States of Chromophores in Polarizable Environment: Orbital Relaxation versus Polarization. *J. Phys. Chem. A* **2010**, *114*, 8824–8830.

(79) Li, Y.-K.; Wu, H.-Y.; Zhu, Q.; Fu, K.-X.; Li, X.-Y. Solvent Effect on the UV/Vis Absorption Spectra in Aqueous Solution: The Nonequilibrium Polarization with An Explicit representation of the Solvent Environment. *J. Chem. Theory Comput.* **2011**, *971*, 65–72.

(80) Aidas, K.; Kongsted, J.; Osted, A.; Mikkelsen, K. V.; Christiansen, O. Coupled Cluster Calculation of the $n \rightarrow \pi^*$ Electronic Transition of Acetone in Aqueous Solution. *J. Phys. Chem. A* **2005**, *109*, 8001–8010.

(81) Gomes, A. S.; Jacob, C. R.; Visscher, L. Calculation of Local Excitations in Large Systems by Embedding Wave-Function Theory in Density-Functional Theory. *Phys. Chem. Chem. Phys.* **2008**, *10*, 5353–5362.

(82) Kaminski, J. W.; Gusarov, S.; Wesolowski, T. A.; Kovalenko, A. Modeling Solva-

tochromic Shifts Using the Orbital-Free Embedding Potential at Statistically Mechanically Averaged Solvent Density. *J. Phys. Chem. A* **2010**, *114*, 6082–6096.

(83) Marenich, A. V.; Cramer, C. J.; Truhlar, D. G. Sorting Out the Relative Contributions of Electrostatic Polarization, Dispersion, and Hydrogen Bonding to Solvatochromic Shifts on Vertical Electronic Excitation Energies. *J. Chem. Theory Comput.* **2010**, *6*, 2829–2844.

(84) Steindal, A. H.; Ruud, K.; Frediani, L.; Aidas, K.; Kongsted, J. Excitation Energies in Solution: The Fully Polarizable QM/MM/PCM Method. *J. Phys. Chem. B* **2011**, *115*, 3027–3037.

(85) Marenich, A. V.; Cramer, C. J.; Truhlar, D. G. Electronic Absorption Spectra and Solvatochromic Shifts by the Vertical Excitation Model: Solvated Clusters and Molecular Dynamics Sampling. *J. Phys. Chem. B* **2015**, *119*, 958–967.

(86) Georg, H. C.; Coutinho, K.; Canuto, S. A Sequential Monte Carlo Quantum Mechanics Study of the Hydrogen-Bond Interaction and the Solvatochromic Shift of the $n - \pi^*$ Transition of Acrolein in Water. *J. Chem. Phys.* **2005**, *123*, 124307.

(87) Aidas, K.; Mogelhoj, A.; Nilsson, E. J.; Johnson, M. S.; Mikkelsen, K. V.; Christiansen, O.; Soderhjelm, P.; Kongsted, J. On the Performance of Quantum Chemical Methods to Predict Solvatochromic Effects: The Case of Acrolein in Aqueous Solution. *J. Chem. Phys.* **2008**, *128*, 194503.

(88) Mata, R. A. Assessing the Accuracy of Many-Body Expansions for the Computation of Solvatochromic Shifts. *Mol. Phys.* **2010**, *108*, 381–392.

(89) Bayliss, N. S.; Wills-Johnson, G. Solvent effects on the Intensities of the Weak Ultraviolet Spectra of Ketones and Nitroparaffins I. *Spectrochim. Acta, Part A* **1968**, *24A*, 551–561.

(90) Xu, H.; Wentworth, P. J.; Howell, N. W.; Joens, J. A. Temperature-Dependent near-UV Molar Absorptivities of Aliphatic-Aldehydes and Ketones in Aqueous-Solution. *Spectrochim. Acta, Part A* **1993**, *49*, 1171–1178.

(91) Balasubramanian, A.; Rao, C. N. R. Evaluation of Solute-Solvent Interactions from Solvent Blue-Shifts of $n \rightarrow \pi^*$ Transitions of C=O, C=S, NO_2 and N=N Groups: Hydrogen Bond Energies of Various Donor-Acceptor Systems. *Spectrochim. Acta, Part A* **1962**, *18*, 1337–1352.

(92) Hayes, W. P.; Timmons, C. J. Solvent and Substituent Effects on $n \rightarrow \pi^*$ Absorption Bands of Some Ketones. *Spectrochim. Acta, Part A* **1965**, *21*, 529–541.

(93) Yudasaka, M.; Hosoya, H. Abnormal Hyperchromism of the $n \rightarrow \pi^*$ Absorption-Band of Acetone in Protic Solvents. *Bull. Chem. Soc. Jpn.* **1978**, *51*, 1708–1713.

(94) Philis, J. G.; Goodman, L. Methyl Rotor Effects on Acetone Rydberg Spectra. II. The $^1B_2(3s \leftarrow n) \leftarrow^1 A_1$ Transition. *J. Chem. Phys.* **1993**, *98*, 3795–3802.

(95) Xing, X.; McDiarmid, R.; Philis, J. G.; Goodman, L. Vibrational Assignments in the $3p$ Rydberg States of Acetone. *J. Chem. Phys.* **1993**, *99*, 7565–7573.

(96) Walsh, A. D. The Absorption Spectra of Acrolein, Crotonaldehyde and Mesityl Oxide in the Vacuum Ultra-Violet. *Trans. Faraday Soc.* **1945**, *41*, 498–505.

(97) Inuzuka, K. Near Ultraviolet Absorption Spectra of Acrolein and Crotonaldehyde. *Bull Chem. Soc. Jpn.* **1960**, *33*, 678–680.

(98) Forbes, W. F.; Shilton, R. Electronic Spectra and Molecular Dimensions. III. Steric Effects in Methyl-Substituted α, β -Unsaturated Aldehydes. *J. Am. Chem. Soc.* **1959**, *81*, 786–790.

(99) Suppan, P. The Influence of the Medium on the Energy of Electronic States. *J. Photochem. Photobiol. A* **1990**, *50*, 293–330.

for Table of Contents use only

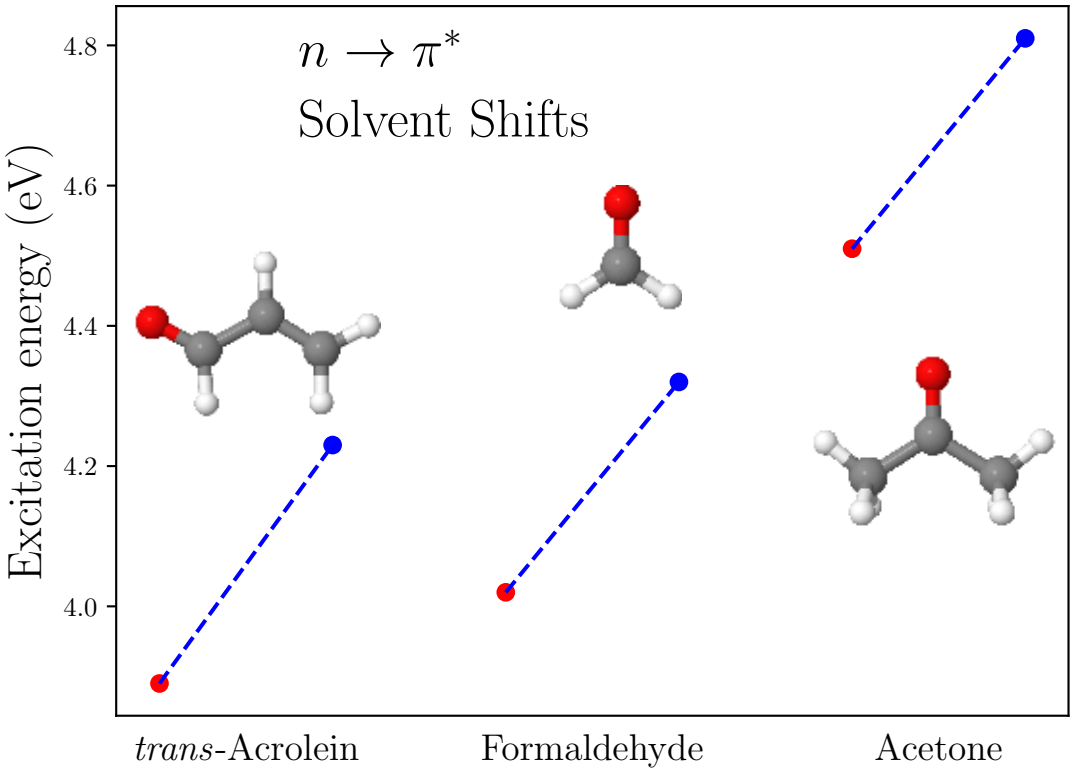

Electronically Excited States in Solution via a Smooth Dielectric Model Combined with Equation-of-Motion Coupled Cluster Theory

J. Coleman Howard, James C. Womack, Jacek Dziedzic ,Chris- Kriton Skylaris, Benjamin P. Pritchard, and T. Daniel Crawford